



Chinese Society of Aeronautics and Astronautics
& Beihang University

Chinese Journal of Aeronautics

cja@buaa.edu.cn
www.sciencedirect.com



Semi-global leader-following consensus-based formation flight of unmanned aerial vehicles



Panpan ZHOU*, Ben M. CHEN

Department of Mechanical and Automation Engineering, The Chinese University of Hong Kong, Hong Kong, China

Received 15 October 2020; revised 28 December 2020; accepted 17 January 2021

Available online 20 March 2021

KEYWORDS

Consensus;
Formation flying;
Input saturation;
Low gain feedback;
Multi-agent systems;
Unmanned aerial vehicles

Abstract In this paper, we investigate a formation control problem of multi-agent systems (specifically a group of unmanned aerial vehicles) based on a semi-global leader-following consensus approach with both the leader and the followers subject to input saturation. Utilizing the low gain feedback design technique, a distributed static control protocol and a distributed adaptive control protocol are constructed. The former solves the problem under an assumption that the communication network is undirected, and it depends on the global information of the graph. For the latter, we relax the undirected graph to directed graph. Moreover, an adaptive updating gain is designed to avoid using the global information of the communication network. It is shown that the consensus protocols can solve the semi-global leader-following consensus problem if the leader agent is globally reachable. The results are verified successfully by both simulation and real flight tests.

© 2021 Chinese Society of Aeronautics and Astronautics. Production and hosting by Elsevier Ltd. This is an open access article under the CC BY-NC-ND license (<http://creativecommons.org/licenses/by-nc-nd/4.0/>).

1. Introduction

Over the last decade, the research of formation control of Unmanned Aerial Vehicles (UAVs) has blossomed due to their potential applications in cooperative payload carrying,¹ surveillance and reconnaissance,² and target search,³ to name a few. The formation control of UAVs can be roughly classified into two categories: analytic solution-based approaches³ and optimization-based approaches.^{4,5} An example of the analytic solution-based approach is consensus-based method, and

one good example of optimization-based approach is Model Predictive Control (MPC). The so-called consensus-based approach means each two of the UAVs keep a constant relative position, and the control protocol is designed in a distributed way, in accordance with the communication topology. In this paper, we adopt the consensus-based approach to address the formation flight of UAVs.

In the previous works, Abdessameud and Tayebi⁶ considered the time-invariant formation problem of UAV swarm systems with communication delays under undirected interaction topologies. Seo et al.⁷ proposed a consensus control law with an output feedback linearization method to deal with the formation problem of a multi-UAV system with partially time-varying formation pattern. The works done by Turpin et al.⁸ achieved planned trajectory given predefined shapes, and real flight tests were given. Dong and Hu⁹ considered the time-varying formation control and containment control for a group of systems with multiple leaders.

* Corresponding author.

E-mail address: ppzhou@mae.cuhk.edu.hk (P. ZHOU).

Peer review under responsibility of Editorial Committee of CJA.



In reality, the trajectory tracking of most UAVs consists of inter-loop control and out-loop control. Provided with the reference position, velocity and acceleration, the inter-loop uses low-level control algorithm, such as PID or LQR, to stabilize the attitude of the vehicle. Thus, with an appropriate inner-loop controller, each UAV can be approximately modeled as a double-integrator system. Recently, the consensus or leader-following consensus problem of linear time-invariant systems have been widely studied.

Semsar-Kazerooni and Khashayar¹⁰ used a semi-decentralized optimal control strategy to accomplish output consensus for both leaderless case and leader-follower case. It is proven that the consensus algorithm is applicable if they follow a predefined topology. Qian et al.¹¹ solved the output consensus problem for heterogeneous linear systems via event-triggered control. It is interesting to find that the works above did not consider the boundedness of control input of agents. In the work of Lin et al.¹² the semi-global output regulation was firstly studied for an individual system subject to input saturation, and a semi-global framework was established. Low gain feedback theory,¹³ parameterized in a scalar low gain parameter, is instrumental in the semi-global output regulation or consensus problem of systems with input saturation. Recently, some results about semi-global consensus of multi-agent systems subject to actuator saturation were obtained via the low gain feedback design technique. In the work of Shi et al.¹⁴ both state feedback and output feedback consensus protocols are constructed. In the output feedback case, a distributed leader state observer and a state observer are designed to estimate the states of the leader and the follower itself. It has shown that these laws achieve the semi-global leader-following output consensus of heterogeneous systems with the follower subject to input saturation if the leader agent is globally reachable. Zhao et al.¹⁵ investigated the semi-global leader-following output consensus of multiple identical linear systems subject to external disturbances and actuator saturation via the output regulation approach. The low-gain feedback-based state-control algorithm is to solve the problem if the topology is a digraph without loop.

In fact, the leader agent with bounded control input is of great importance as it can generate safe trajectories to avoid obstacles. However, the above results did not take the input of the leader agent into consideration. In this paper, we study the semi-global leader-following consensus-based formation control of a multi-UAV system. The contribution of this paper is twofold. First, the leader agent has control input, and it is subject to saturation. If the leader has zero control input, its trajectory is fixed once given the initial condition. The control input provides a freedom for the leader to generate trajectories to response to external environment, so that it can reach to the destination safely. Second, based on the low gain design technique, a distributed static control protocol and a distributed adaptive control protocol are constructed. The distributed static control protocol requires the global information of the communication undirected graph, while in the distributed adaptive control protocol, the graph is relaxed from undirected graph to directed graph. More importantly, an updating gain is proposed so that the control law is independent of the communication graph. The results are verified by both simulation and real indoor flight tests.

The reminder of this paper is organized as follows. Section 2 gives the problem formulation, after which, the proposed dis-

tributed static control and distributed adaptive control are constructed in Section 3.1 and Section 3.2, respectively. In Section 3.3, we formulate a formation problem of UAVs into the consensus problem. In Section 4, both simulation and real flight test of UAVs are given to verify the effectiveness of the two control protocols. Finally, we conclude our work with some remarks in Section 5.

Notation: X^T denotes the transpose of the matrix or vector X . For a time constant $t \geq 0$ and a signal $x: \mathbf{R}_+ \rightarrow \mathbf{R}^s$, $x = [x_1, x_2, \dots, x_s]^T$, $\|x\|$ denotes the Euclidean norm, $\|x\|_\infty = \max_i |x_i|$ and $\|x\|_{t,\infty} = \sup_{t \geq 0} \|x\|$. $\mathbf{1}_N \in \mathbf{R}^N$ represents an N -dimensional column vector with all entries being 1. I_N denotes an N -dimensional identity matrix. \otimes represents the Kronecker product. $R_{\text{odd}}^+ = \{x \in \mathbf{R} : x > 0 \text{ and } x \text{ is a ratio of odd integers}\}$.

2. Problem formulation

Currently, the majority of autonomous unmanned aerial systems have a hierarchical framework to track a trajectory, as depicted in Fig. 1. Different algorithms are used in the trajectory generator block to provide reference information, such as position, velocity and acceleration, to the lower-level flight control system, which itself generally consists of two layers, i.e., the inner-loop and the outer-loop controller. The inner-loop control law is to stabilize the attitude of the unmanned vehicle. A properly designed inner-loop controller would render the dynamics of the vehicle to behave like a point mass and thus it can be approximated by a double integrator, which can be utilized to design an outer-loop control to track the references generated from the trajectory generator (see e.g., Cai et al.¹⁶). This hierarchic method promotes us to be more attentive to trajectory generation algorithms without paying much attention to the low-level system. In this paper, we use the consensus-based algorithm to generate references for all UAVs in the multi-UAV system.

Consider a group of $N + 1$ UAVs labeled $0, 1, \dots, N$, each of which is modeled as a double-integrator system, and the problem is considered in a 2-D plane or a 3-D plane. Their dynamics are described as

$$\begin{cases} \dot{p}_i = v_i \\ \dot{v}_i = a_i \end{cases} \quad i = 0, 1, \dots, N \quad (1)$$

where $p_i \in \mathbf{R}^2$ or $p_i \in \mathbf{R}^3$, v_i and a_i represent the position, velocity and acceleration of the i th UAV, respectively. It is obvious that systems can be represented by time-invariant systems

$$\dot{x}_i = Ax_i + B\sigma_{\Delta_i}(u_i) \quad i = 0, 1, \dots, N \quad (2)$$

where $x_i = p_i$, $u_i = v_i$, or $x_i = [p_i^T, v_i^T]^T$, $u_i = a_i$. To generalize the problem, we assume $x_i \in \mathbf{R}^n$, $u_i \in \mathbf{R}^m$. $\sigma_{\Delta}: \mathbf{R}^m \rightarrow \mathbf{R}^m$ denotes a vector valued saturation function, that is, for $s = [s_1, s_2, \dots, s_m]^T$, $\sigma_{\Delta}(s) = [\sigma_{\Delta}(s_1), \sigma_{\Delta}(s_2), \dots, \sigma_{\Delta}(s_m)]^T$ and

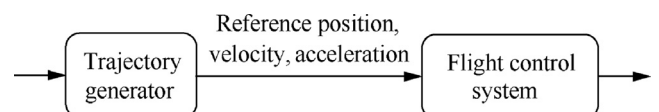


Fig. 1 Trajectory tracking of a single UAV.

for each $j = 1, 2, \dots, m$, $\sigma_\Delta(s_j) = \text{sgn}(s_j) \min\{|s_j|, \Delta\}$, where $\Delta > 0$ is a constant. For simplicity, we use γ to represent the input bound of the leader UAV, and assume that the follower UAVs have the same input bound Δ , that is, $\gamma = \Delta_0$, and $\Delta = \Delta_1 = \Delta_2 = \dots = \Delta_N$. Therefore, the control input of each UAV is subject to saturation.

The communication topology among the UAVs is presented by the graph $\mathcal{G} = \{\mathcal{V}, \mathcal{E}\}$, with $\mathcal{V} = \{0, 1, \dots, N\}$ and $\mathcal{E} = \mathcal{V} \times \mathcal{V}$ representing the node set and the edge set. For $i, j \in \mathcal{V}$, $(j, i) \in \mathcal{E}$ if and only if UAV i can receive the information of UAV j , and we say UAV j is a neighbor of UAV i , and UAV i is a child of UAV j . We use \mathcal{N}_i to denote the set of neighbors of UAV i , that is, $\mathcal{N}_i := \{j : (j, i) \in \mathcal{E}\}$. The graph is called undirected if $(j, i) \in \mathcal{E}$ implies $(i, j) \in \mathcal{E}$. Without loss of generality, we assume the node 0 is the leader UAV and the rest N UAVs are the followers which is denoted by $\mathcal{F} = \{1, 2, \dots, N\}$. If there is a sequence of edges $(i_1, i_2), (i_2, i_3), \dots, (i_{k-1}, i_k)$, then we say there is a direct path from i_1 to i_k , or i_k is reachable from i_1 . In our work, we assume that the leader can-not obtain the information of the followers. For a graph \mathcal{G} , the adjacency matrix $\mathbf{A} = [a_{ij}] \in \mathbf{R}^{(N+1) \times (N+1)}$ is defined as $a_{ij} = 1$ if $(j, i) \in \mathcal{E}$, otherwise, $a_{ij} = 0$. The Laplacian matrix $\mathbf{L} = [l_{ij}] \in \mathbf{R}^{(N+1) \times (N+1)}$ is defined as $l_{ij} = -a_{ij}$ if $i \neq j$, and $l_{ii} = \sum_{j=0}^N a_{ij}$. According to the classification of the leader UAV and the follower UAVs, the Laplacian matrix can be rewritten as $\mathbf{L} = \begin{bmatrix} 0 & \mathbf{0}_{1 \times N} \\ \mathbf{L}_2 & \mathbf{L}_1 \end{bmatrix}$, where $\mathbf{L}_2 \in \mathbf{R}^{N \times 1}$ and $\mathbf{L}_1 \in \mathbf{R}^{N \times N}$.

In this paper, we firstly solve the semi-global leader-following consensus problem of multi-agent linear systems with input saturation. We will then formulate a formation control problem of multiple UAVs as the consensus problem. Via the consensus-based approach, a reference trajectory for each UAV will be generated for them to track.

Problem 1. Consider the multi-UAV systems in Eq. (2). Let $\mathbf{x}_f = [\mathbf{x}_1^T, \mathbf{x}_2^T, \dots, \mathbf{x}_N^T]^T$. For any a priori given bounded set $\mathcal{X}_{f,0} \in \mathbf{R}^{nN}$, design a state feedback control protocol $\mathbf{u}_i = h_i(\mathbf{x}_i, \mathbf{x}_j, j \in \mathcal{N}_i)$ such that the resulting closed-loop multi-UAV systems in Eq. (2) achieves leader-following state consensus on $\mathcal{X}_{f,0} \times \mathcal{X}_{0,0}$, that is, for $[\mathbf{x}_f^T(0), \mathbf{x}_0^T(0)]^T \in \mathcal{X}_{f,0} \times \mathcal{X}_{0,0}$, the leader-following state consensus error $\mathbf{e}_i = \mathbf{x}_i - \mathbf{x}_0$ satisfies $\lim_{t \rightarrow \infty} \mathbf{e}_i = \mathbf{0}$.

To solve **Problem 1**, the following assumptions are required.

Assumption 1. The pair (\mathbf{A}, \mathbf{B}) is stabilizable, and all eigenvalues of \mathbf{A} are located in the closed left-half complex plane.

Assumption 2. The input bound of the leader UAV γ is less than the input bound of the follower UAVs, that is, $\gamma < \Delta$.

Assumption 3. Every follower is reachable from the leader UAV, and the communication topology among the followers is undirected.

Remark 1. Assumptions 1 and 3 are widely used in the study of consensus control of multi-agent systems. Under **Assumption 3**, \mathbf{L}_1 is symmetric, and all eigenvalues of \mathbf{L}_1 are positive.¹⁷ In the following part, we will show that **Assumption 2** is necessary for solving the proposed problem. If the input bound of the leader is larger than the input bound of the followers, it is impossible for the followers to catch up the leader when it moves at its maximal pace. Moreover, we assume that the input bound of the leader UAV γ is only known to the followers who are the children of the leader UAV.

Recall the following parameterized Algebraic Riccati Equation (ARE), based on which the low-gain state feedback control law is designed.

Lemma 1. (see Lin¹³) Let **Assumption 1** hold. Then, for each $\varepsilon \in (0, 1]$, there exists a unique positive-definite solution $\mathbf{P}(\varepsilon) \in \mathbf{R}^{n \times n}$ that satisfies

$$\mathbf{A}^T \mathbf{P}(\varepsilon) + \mathbf{P}(\varepsilon) \mathbf{A} - \mathbf{P}(\varepsilon) \mathbf{B} \mathbf{B}^T \mathbf{P}(\varepsilon) = -\varepsilon \mathbf{I}_n \quad (3)$$

and $\lim_{\varepsilon \rightarrow 0} \mathbf{P}(\varepsilon) = \mathbf{0}$.

The low-gain feedback design technique in Lin¹³ was originally designed for linear systems with input saturation to solve the semi-global stabilization problem. By selecting ε small enough, for any a priori given, arbitrarily large and bounded set of initial condition, the low gain feedback law guarantees the control input to be unsaturated. In the following section, two consensus protocols are constructed based on the low-gain feedback design technique.

3. Main results

In this section, based on the aforementioned low-gain feedback design technique, two distributed state-feedback control protocols are designed. The first control law requires a priori given global information of the communication graph, while the second one is fully distributed, i.e., it is constructed only using the information of its neighbors. Let $\mathbf{P}(\varepsilon) > \mathbf{0}$ be the solution of the parameterized ARE in Eq. (3). For convenience, we denote $\mathbf{P} = \mathbf{P}(\varepsilon)$ hereafter.

In our problem, we assume the input bound of the leader UAV γ is only known to part of the follower UAVs, so a distributed observer is designed to estimate γ .

For $i \in \mathcal{F}$,

$$\dot{\gamma}_i = -\mu_1 \left(\sum_{j \in \mathcal{F}} a_{ij} (\gamma_i - \gamma_j) + a_{i0} (\gamma_i - \gamma) \right)^\rho \quad (4)$$

where μ_1 and ρ are constants with $\mu_1 > 0$, $1/2 < \rho < 1$ and $\rho \in \mathbf{R}_{\text{odd}}^+$. It has been shown that $\gamma_i \rightarrow \gamma$ in finite time.¹⁸

3.1. Consensus with distributed static control

Consider the following dynamic compensator for follower i , $i = 1, 2, \dots, N$,

$$\mathbf{u}_i = -\mu_2 \mathbf{B}^T \mathbf{P} \left(\sum_{j=1}^N a_{ij} (\mathbf{x}_i - \mathbf{x}_j) + a_{i0} (\mathbf{x}_i - \mathbf{x}_0) \right) - \gamma \mathbf{f}_i(t) \quad (5)$$

where $\mu_2 \geq 1/(2\lambda_{\min}(\mathbf{L}_1))$ is a positive scalar. Let $\zeta_i(t) = \sum_{j=1}^N a_{ij}(\mathbf{x}_i - \mathbf{x}_j) + a_{i0}(\mathbf{x}_i - \mathbf{x}_0)$, $\mathbf{f}_i(t)$ is defined as

$$\mathbf{f}_i(t) = \begin{cases} \frac{\mathbf{B}^T \mathbf{P} \zeta_i(t)}{\|\mathbf{B}^T \mathbf{P} \zeta_i(t)\|}, & \text{if } \zeta_i(t) \neq \mathbf{0} \\ \mathbf{0}, & \text{otherwise} \end{cases} \quad (6)$$

We note that $\|\mathbf{f}_i(t)\| = 1$ or 0 .

Theorem 1. Consider the multi-UAV systems in Eq. (2). Let Assumptions 1–3 hold. **Problem 1** is solved by the low-gain control protocol (5). That is, for any a priori given bounded sets $\mathcal{X}_{f,0} \in \mathbf{R}^{nN}$ and $\mathcal{X}_{0,0} \in \mathbf{R}^n$, there is an $\varepsilon^* \in (0, 1]$, such that for any $\varepsilon \in (0, \varepsilon^*)$, and $[\mathbf{x}_f^T(0), \mathbf{x}_0^T(0)]^T \in \mathcal{X}_{f,0} \times \mathcal{X}_{0,0}$, the leader-following consensus error satisfies $\lim_{t \rightarrow \infty} \mathbf{e}_i = \mathbf{0}$.

Proof. Define $\tilde{\mathbf{x}}_i(t) = \mathbf{x}_i(t) - \mathbf{x}_0(t)$, $\tilde{\mathbf{x}}_f(t) = [\tilde{\mathbf{x}}_1^T(t), \tilde{\mathbf{x}}_2^T(t), \dots, \tilde{\mathbf{x}}_n^T(t)]^T$, and $\zeta(t) = [\zeta_1^T(t), \zeta_2^T(t), \dots, \zeta_n^T(t)]^T$. We note $\zeta(t) = (\mathbf{L}_1 \otimes \mathbf{I}_n) \tilde{\mathbf{x}}_f(t)$. Next, the closed-loop system is rewritten in terms of the new state $\zeta(t)$. The asymptotic convergence to zero of $\zeta(t)$ implies the asymptotic convergence to zero of $\tilde{\mathbf{x}}_f(t)$, and thus the consensus problem is solved.

Since $\gamma_i \rightarrow \gamma$ in finite time, there exists a time t_1 such that for $t \geq t_1$, $\gamma_i \equiv \gamma$. Then, it follows that, for $t \geq t_1$, the control protocol can be written as

$$\mathbf{u}_i = -\mu_2 \mathbf{B}^T \mathbf{P} \left(\sum_{j=1}^N a_{ij}(\mathbf{x}_i - \mathbf{x}_j) + a_{i0}(\mathbf{x}_i - \mathbf{x}_0) \right) - \gamma \mathbf{f}_i(t) \quad (7)$$

Substituting the control protocol (7) into (2) gives

$$\begin{aligned} \dot{\mathbf{x}}_i &= \mathbf{A} \mathbf{x}_i \\ &+ \mathbf{B} \sigma_{\Delta} \left(-\mu_2 \mathbf{B}^T \mathbf{P} \left(\sum_{j=1}^N a_{ij}(\mathbf{x}_i - \mathbf{x}_j) + a_{i0}(\mathbf{x}_i - \mathbf{x}_0) \right) - \gamma \mathbf{f}_i(t) \right) \end{aligned} \quad (8)$$

Notice that for $i \in \mathcal{F}$, and $t_2 \geq t_1$, $\mathbf{x}_i(t_2) \in \mathcal{X}_{i,T_2}$ and $\mathbf{x}_0(t_2) \in \mathcal{X}_{0,T_2}$ for some bounded sets \mathcal{X}_{i,T_2} and \mathcal{X}_{0,T_2} , which are independent of ε , because $\mathbf{x}_i(0)$ and $\mathbf{x}_0(0)$ are bounded, and $\mathbf{x}_i(0)$, $\mathbf{x}_0(0)$ are determined by linear time-invariant equations with bounded input $\sigma_{\Delta}(\mathbf{u}_i)$ and $\sigma_{\gamma}(\mathbf{u}_0)$, respectively. Therefore, $\zeta(t_2) \in \mathcal{X}_{\zeta,T_2}$ for some bounded set \mathcal{X}_{ζ,T_2} .

Next, we construct the following Lyapunov function candidate

$$V_{\zeta}(t) = \zeta^T (\mathbf{I}_N \otimes \mathbf{P}) \zeta \quad (9)$$

where \mathbf{P} is the solution of the ARE.

Let $c_1 > 0$ be a constant such that

$$\sup_{\mathbf{x}_i(t_2) \in \mathcal{X}_{i,T_2}, \mathbf{x}_0(t_2) \in \mathcal{X}_{0,T_2}, \varepsilon \in (0,1]} V_{\zeta}(t) \leq c_1$$

Such a c_1 exists because \mathcal{X}_{i,T_2} and \mathcal{X}_{0,T_2} are bounded. Define $L_V(c_1) := \{\zeta \in \mathbf{R}^{nN} : V_{\zeta}(t) \leq c_1\}$. Since $L_V(c_1)$ is bounded and $\lim_{\varepsilon \rightarrow 0} \mathbf{P}(\varepsilon) = \mathbf{0}$, there exists an $\varepsilon^* \in (0, 1]$ such that for all $\varepsilon \in (0, \varepsilon^*)$, $\zeta \in L_V(c_1)$ implies that

$$\begin{aligned} &\left\| -\mu_2 \mathbf{B}^T \mathbf{P} \left[\sum_{j=1}^N a_{ij}(\mathbf{x}_i - \mathbf{x}_j) + a_{i0}(\mathbf{x}_i - \mathbf{x}_0) \right] \right\|_{\infty, t_2} \\ &= \left\| -\mu_2 \mathbf{B}^T \mathbf{P} \zeta_i(t) \right\|_{\infty, t_2} \leq \Delta - \gamma \end{aligned} \quad (10)$$

Then, by Eq. (10) and the fact that $\|\mathbf{f}_i(t)\| = 1$ or 0 , we have

$$\begin{aligned} \|\mathbf{u}_i\|_{\infty, t_2} &= \left\| -\mu_2 \mathbf{B}^T \mathbf{P} \zeta_i(t) - \gamma \mathbf{f}_i(t) \right\|_{\infty, t_2} \\ &\leq \left\| \mu_2 \mathbf{B}^T \mathbf{P} \zeta_i(t) \right\|_{\infty, t_2} + \left\| \gamma \mathbf{f}_i(t) \right\|_{\infty, t_2} \leq (\Delta - \gamma) + \gamma \\ &= \Delta \end{aligned}$$

Thus, $\sigma_{\Delta}(\mathbf{u}_i) = \mathbf{u}_i$.

Therefore, the closed-loop system can be rewritten as

$$\dot{\mathbf{x}}_i = \mathbf{A} \mathbf{x}_i - \mu_2 \mathbf{B} \mathbf{B}^T \mathbf{P} \zeta_i(t) - \gamma \mathbf{B} \mathbf{f}_i(t), \quad i \in \mathcal{F}$$

It follows that

$$\dot{\mathbf{x}}_f = (\mathbf{I}_N \otimes \mathbf{A}) \mathbf{x}_f - \mu_2 (\mathbf{I}_N \otimes \mathbf{B} \mathbf{B}^T \mathbf{P}) \zeta(t) - \gamma (\mathbf{I}_N \otimes \mathbf{B}) \bar{\mathbf{f}}(t)$$

with $\bar{\mathbf{f}}(t) = [\mathbf{f}_1^T(t), \mathbf{f}_2^T(t), \dots, \mathbf{f}_n^T(t)]^T$. Define $\bar{\mathbf{x}}_0(t) = \mathbf{1}_N \otimes \mathbf{x}_0(t)$, and $\sigma_{\gamma}(\bar{\mathbf{u}}_0) = \mathbf{1}_N \otimes \sigma_{\gamma}(\mathbf{u}_0)$, we have

$$\begin{aligned} \dot{\bar{\mathbf{x}}}_f &= \dot{\mathbf{x}}_f - \dot{\bar{\mathbf{x}}}_0 \\ &= (\mathbf{I}_N \otimes \mathbf{A}) \tilde{\mathbf{x}}_f - \mu_2 (\mathbf{I}_N \otimes \mathbf{B} \mathbf{B}^T \mathbf{P}) \zeta(t) - \gamma (\mathbf{I}_N \otimes \mathbf{B}) \bar{\mathbf{f}}(t) \\ &\quad - (\mathbf{I}_N \otimes \mathbf{B}) \sigma_{\gamma}(\bar{\mathbf{u}}_0) \end{aligned}$$

Since $\zeta(t) = (\mathbf{L}_1 \otimes \mathbf{I}_n) \tilde{\mathbf{x}}_f(t)$, it gives that

$$\begin{aligned} \dot{\zeta}(t) &= (\mathbf{L}_1 \otimes \mathbf{I}_n) \dot{\tilde{\mathbf{x}}}_f(t) \\ &= (\mathbf{L}_1 \otimes \mathbf{A}) \tilde{\mathbf{x}}_f(t) - \mu_2 (\mathbf{L}_1 \otimes \mathbf{B} \mathbf{B}^T \mathbf{P}) \zeta(t) - \gamma (\mathbf{L}_1 \otimes \mathbf{B}) \bar{\mathbf{f}}(t) \\ &\quad - (\mathbf{L}_1 \otimes \mathbf{B}) \sigma_{\gamma}(\bar{\mathbf{u}}_0) \\ &= (\mathbf{L}_1 \otimes \mathbf{A}) (\mathbf{L}_1^{-1} \otimes \mathbf{I}_n) \zeta(t) - \mu_2 (\mathbf{L}_1 \otimes \mathbf{B} \mathbf{B}^T \mathbf{P}) \zeta(t) \\ &\quad - \gamma (\mathbf{L}_1 \otimes \mathbf{B}) \bar{\mathbf{f}}(t) - (\mathbf{L}_1 \otimes \mathbf{B}) \sigma_{\gamma}(\bar{\mathbf{u}}_0) \\ &= [\mathbf{I}_N \otimes \mathbf{A} - \mu_2 (\mathbf{L}_1 \otimes \mathbf{B} \mathbf{B}^T \mathbf{P})] \zeta(t) - \gamma (\mathbf{L}_1 \otimes \mathbf{B}) \bar{\mathbf{f}}(t) \\ &\quad - (\mathbf{L}_1 \otimes \mathbf{B}) \sigma_{\gamma}(\bar{\mathbf{u}}_0) \end{aligned}$$

Given the Lyapunov function in Eq. (10), the derivative satisfies

$$\begin{aligned} \dot{V}_{\zeta}(t) &= \zeta^T [\mathbf{I}_N \otimes \mathbf{A} - \mu_2 (\mathbf{L}_1 \otimes \mathbf{B} \mathbf{B}^T \mathbf{P})]^T (\mathbf{I}_N \otimes \mathbf{P}) \zeta \\ &\quad + \zeta^T (\mathbf{I}_N \otimes \mathbf{P}) [\mathbf{I}_N \otimes \mathbf{A} - \mu_2 (\mathbf{L}_1 \otimes \mathbf{B} \mathbf{B}^T \mathbf{P})] \zeta \\ &\quad - 2\gamma \zeta^T (\mathbf{I}_N \otimes \mathbf{P}) (\mathbf{L}_1 \otimes \mathbf{B}) \bar{\mathbf{f}}(t) - 2\gamma \zeta^T (\mathbf{I}_N \otimes \mathbf{P}) \\ &\quad \times (\mathbf{L}_1 \otimes \mathbf{B}) \sigma_{\gamma}(\bar{\mathbf{u}}_0) \\ &= \zeta^T [\mathbf{I}_N \otimes (\mathbf{A}^T \mathbf{P} + \mathbf{P} \mathbf{A}) - \mu_2 (\mathbf{L}_1^T + \mathbf{L}_1) \otimes \mathbf{P} \mathbf{B} \mathbf{B}^T \mathbf{P}] \zeta \\ &\quad - 2\gamma \zeta^T (\mathbf{L}_1 \otimes \mathbf{P} \mathbf{B}) \bar{\mathbf{f}}(t) - 2\gamma \zeta^T (\mathbf{L}_1 \otimes \mathbf{P} \mathbf{B}) \sigma_{\gamma}(\bar{\mathbf{u}}_0) \end{aligned} \quad (11)$$

We note that

$$\begin{aligned} &\mathbf{I}_N \otimes (\mathbf{A}^T \mathbf{P} + \mathbf{P} \mathbf{A}) - \mu_2 (\mathbf{L}_1^T + \mathbf{L}_1) \otimes \mathbf{P} \mathbf{B} \mathbf{B}^T \mathbf{P} \leq \mathbf{I}_N \\ &\quad \otimes (\mathbf{A}^T \mathbf{P} + \mathbf{P} \mathbf{A} - 2\mu_2 \lambda_{\min}(\mathbf{L}_1) \mathbf{P} \mathbf{B} \mathbf{B}^T \mathbf{P}) \\ &\leq \mathbf{I}_N \otimes (\mathbf{A}^T \mathbf{P} + \mathbf{P} \mathbf{A} - \mathbf{P} \mathbf{B} \mathbf{B}^T \mathbf{P}) \\ &= -\mathbf{I}_N \otimes \varepsilon \mathbf{I}_n \end{aligned} \quad (12)$$

The last inequality holds if μ_2 is chosen large enough such that $\mu_2 \geq 1/(2\lambda_{\min}(\mathbf{L}_1))$

On the other hand, according to the definition of $\mathbf{f}_i(t)$ in Eq. (6), we can obtain that $\zeta_i^T(t) \mathbf{P} \mathbf{B} \mathbf{f}_i(t) = \|\mathbf{B}^T \mathbf{P} \zeta_i(t)\|$ and $\zeta_i^T(t) \mathbf{P} \mathbf{B} \mathbf{f}_j(t) \leq \|\mathbf{B}^T \mathbf{P} \zeta_i(t)\|$. Then, it follows that

$$\begin{aligned}
-2\gamma\zeta^T(\mathbf{L}_1 \otimes \mathbf{P}\mathbf{B})\bar{\mathbf{f}}(t) &= 2\gamma\sum_{i=1}^N\zeta_i^T\mathbf{P}\mathbf{B}\left(\sum_{j\in\mathcal{F}}a_{ij}(\mathbf{f}_j(t)-\mathbf{f}_i(t))-a_{i0}\mathbf{f}_i(t)\right) \\
&\leq -2\gamma\sum_{i=1}^N\zeta_i^T\mathbf{P}\mathbf{B}\cdot a_{i0}\mathbf{f}_i(t) = -2\gamma\sum_{i=1}^Na_{i0}\|\zeta_i^T\mathbf{P}\mathbf{B}\|
\end{aligned} \tag{13}$$

and

$$\begin{aligned}
-2\gamma\zeta^T(\mathbf{L}_1 \otimes \mathbf{P}\mathbf{B})\sigma_\gamma(\bar{\mathbf{u}}_0) &= 2\sum_{i=1}^N\zeta_i^T\mathbf{P}\mathbf{B}\cdot a_{i0}\sigma_\gamma(\mathbf{u}_0) \\
&\leq 2\gamma\sum_{i=1}^Na_{i0}\|\zeta_i^T\mathbf{P}\mathbf{B}\|
\end{aligned} \tag{14}$$

Substituting Eqs. (12)–(14), into Eq. (11) gives

$$\begin{aligned}
\dot{V}_\zeta(t) &\leq \zeta^T(-\mathbf{I}_N \otimes \varepsilon\mathbf{L}_n)\zeta - 2\gamma\sum_{i=1}^Na_{i0}\|\zeta_i^T\mathbf{P}\mathbf{B}\| + 2\gamma\sum_{i=1}^Na_{i0}\|\zeta_i^T\mathbf{P}\mathbf{B}\| \\
&\leq -\zeta^T(\mathbf{I}_N \otimes \varepsilon\mathbf{L}_n)\zeta
\end{aligned}$$

Since $\dot{V}_\zeta(t) \equiv 0$ leads to $\zeta(t) = \mathbf{0}$, thus, it holds that $\lim_{t \rightarrow \infty} \zeta(t) = \mathbf{0}$, which implies that $\lim_{t \rightarrow \infty} (\mathbf{x}_i(t) - \mathbf{x}_0(t)) = \mathbf{0}$.

This completes the proof. ■

3.2. Consensus with distributed adaptive control

In the previous subsection, the design of the control protocol (5) is based on the precondition of the minimal eigenvalue $\lambda_{\min}(\mathbf{L}_1)$ of \mathbf{L}_1 , and it is only applicable to undirected communication graph. However, it is difficult to determine $\lambda_{\min}(\mathbf{L}_1)$ when the network of the multi-UAV systems is of a large scale. In this subsection, we aim to solve the consensus problem without using the global information of the graph and the communication network is relaxed from undirected graph to directed graph.

Assumption 4. Every follower is reachable from the leader UAV, and the communication topology among the followers is directed.

Lemma 2. (see Qu¹⁹) Under **Assumption 4**, all eigenvalues of \mathbf{L}_1 have positive real parts. Moreover, there exists a diagonal matrix $\mathbf{D} = \text{diag}\{d_1, d_2, \dots, d_N\}$ with $d_i > 0$, ($i = 1, 2, \dots, N$) such that $\bar{\mathbf{L}}_1 = \mathbf{D}\mathbf{L}_1 + \mathbf{L}_1^T\mathbf{D} > \mathbf{0}$.

Consider the following consensus protocol for follower i , $i \in \mathcal{F}$,

$$\mathbf{u}_i = -\mathbf{B}^T\mathbf{P}(\alpha_i(t) + \zeta_i^T(t)\mathbf{P}\zeta_i(t))\zeta_i(t) - \gamma_i\mathbf{g}_i(t) \tag{15}$$

where γ_i is the state in the distributed observer (4); $\zeta_i(t) = \sum_{j=1}^Na_{ij}(\mathbf{x}_i - \mathbf{x}_j) + a_{i0}(\mathbf{x}_i - \mathbf{x}_0)$; $\alpha_i(t)$ is the adaptive updating gain to avoid using the global information of the communication graph with $\alpha_i(0) > 0$, and it is updated by

$$\dot{\alpha}_i(t) = \zeta_i^T(t)\mathbf{P}\mathbf{B}\mathbf{B}^T\mathbf{P}\zeta_i(t) \tag{16}$$

$\mathbf{g}_i(t)$ is defined as

$$\mathbf{g}_i(t) = \begin{cases} \frac{\mathbf{B}^T\mathbf{P}\zeta_i(t)}{\|\mathbf{B}^T\mathbf{P}\zeta_i(t)\|}, & \text{if } \zeta_i(t) \neq \mathbf{0} \\ \mathbf{0}, & \text{otherwise} \end{cases} \tag{17}$$

Theorem 2. Consider the multi-UAV systems in Eq. (2). Let Assumptions 1, 2 and 4 hold. Then, **Problem 1** is solved by the low-gain control protocol (15). That is, for any a priori given bounded sets $\mathcal{X}_{t,0} \in \mathbf{R}^{nN}$ and $\mathcal{X}_{0,0} \in \mathbf{R}^n$, there is an $\varepsilon^* \in (0, 1]$, such that for any $\varepsilon \in (0, \varepsilon^*]$, and $[\mathbf{x}_f^T(0), \mathbf{x}_0^T(0)]^T \in \mathcal{X}_{t,0} \times \mathcal{X}_{0,0}$, the leader-following consensus error satisfies $\lim_{t \rightarrow \infty} \mathbf{e}_i = \mathbf{0}$.

Proof. Since $\gamma_i \rightarrow \gamma$ in finite time, there exists a time t_1 such that for $t \geq t_1$, $\gamma_i \equiv \gamma$, i.e., $\tilde{\gamma}_i := \gamma_i - \gamma \equiv 0$ when $t \geq t_1$. Denote $\varphi_i(t) = \alpha_i(t) + \zeta_i^T(t)\mathbf{P}\zeta_i(t)$, it follows that

$$\mathbf{u}_i = -\mathbf{B}^T\mathbf{P}\varphi_i(t)\zeta_i(t) - \gamma_i\mathbf{g}_i(t)$$

Note that for $T_3 \geq T_1$, $\zeta_i(T_3) \in \mathcal{X}_{\zeta_i, T_3}$, $\alpha_i(T_3) \in \mathcal{X}_{\alpha_i, T_3}$ for some bounded sets $\mathcal{X}_{\zeta_i, T_3}$ and $\mathcal{X}_{\alpha_i, T_3}$, which are independent of ε , thus $\varphi_i(t_3) \in \mathcal{X}_{\varphi_i, T_3}$ for a bounded set $\mathcal{X}_{\varphi_i, T_3}$.

Next, we construct the following Lyapunov function candidate

$$V_\zeta = \frac{1}{2}\sum_{i=1}^Nd_i[\varphi_i(t) + \alpha_i(t)]\zeta_i^T(t)\mathbf{P}\zeta_i(t) + \frac{1}{2}\sum_{i=1}^Nd_i\tilde{\alpha}_i^2(t) \tag{18}$$

where d_i is defined in **Lemma 2**, \mathbf{P} is the solution of the ARE (3), and $\tilde{\alpha}_i(t) = \alpha_i(t) - \alpha$ with α denoting a positive constant to be determined.

Let $c_2 > 0$ be a constant such that

$$\sup_{\varphi_i(T_3) \in \mathcal{X}_{\varphi_i, T_3}, \zeta_i(T_3) \in \mathcal{X}_{\zeta_i, T_3}, \alpha_i(T_3) \in \mathcal{X}_{\alpha_i, T_3}, \varepsilon \in (0, 1]} V_\zeta(\cdot) \leq c_2$$

Such a c_2 exists because sets $\mathcal{X}_{\varphi_i, T_3}$, $\mathcal{X}_{\zeta_i, T_3}$ and $\mathcal{X}_{\alpha_i, T_3}$ are bounded. Define

$$L_V(c_2) := \left\{ \begin{bmatrix} \zeta \\ \alpha \end{bmatrix} \in \mathbf{R}^{nN+N} : V_\zeta(t) \leq c_2 \right\}$$

Let $\varepsilon_2^* \in (0, 1]$ be such that for all $\varepsilon \in (0, \varepsilon_2^*]$, $[\zeta^T, \alpha^T]^T \in L_V(c_2)$, which implies that

$$\|-\mathbf{B}^T\mathbf{P}\varphi_i(t)\zeta_i(t)\|_{\infty, t_3} \leq \Delta - \gamma$$

The existence of such an ε_2^* follows the fact $\lim_{\varepsilon \rightarrow 0} \mathbf{P}(\varepsilon) = \mathbf{0}$.

Thus, we have

$$\begin{aligned}
\|\mathbf{u}_i\|_{\infty, t_3} &= \|-\mathbf{B}^T\mathbf{P}\varphi_i(t)\zeta_i(t) - \gamma_i\mathbf{g}_i(t)\|_{\infty, t_3} \\
&\leq \|-\mathbf{B}^T\mathbf{P}\varphi_i(t)\zeta_i(t)\|_{\infty, t_3} + \|\gamma_i\mathbf{g}_i(t)\|_{\infty, t_3} \\
&\leq \Delta - \gamma + \gamma \\
&\leq \Delta
\end{aligned}$$

which means $\sigma_\Delta(\mathbf{u}_i) = \mathbf{u}_i$. Applying the control protocol to the given system gives

$$\dot{\mathbf{x}}_i = \mathbf{A}\mathbf{x}_i - \mathbf{B}\mathbf{B}^T\mathbf{P}\varphi_i(t)\zeta_i(t) - \gamma\mathbf{B}\mathbf{g}_i(t)$$

Since $\zeta(t) = (\mathbf{L}_1 \otimes \mathbf{I}_n)\tilde{\mathbf{x}}_r(t)$, $\zeta(t)$ is determined by the following equation

$$\begin{aligned}
\dot{\zeta}(t) &= (\mathbf{I}_N \otimes \mathbf{A})\zeta(t) - (\mathbf{L}_1\phi(t) \otimes \mathbf{B}\mathbf{B}^T\mathbf{P})\zeta(t) \\
&\quad - \gamma(\mathbf{L}_1 \otimes \mathbf{B})\mathbf{g}(t) - (\mathbf{L}_1 \otimes \mathbf{B})\sigma_\gamma(\bar{\mathbf{u}}_0)
\end{aligned} \tag{19}$$

where $\phi(t) = \text{diag}\{\varphi_1(t), \varphi_2(t), \dots, \varphi_N(t)\}$.

Then, the derivative of the Lyapunov function in Eq. (18) satisfies

$$\begin{aligned}
\dot{V}_\zeta(t) &= \boldsymbol{\omega}_1(t) + \boldsymbol{\omega}_2(t) \\
&= 2\sum_{i=1}^Nd_i\varphi_i(t)\zeta_i^T(t)\mathbf{P}\dot{\zeta}_i(t) + \sum_{i=1}^Nd_i[\varphi_i(t) - \alpha]\dot{\alpha}_i(t)
\end{aligned}$$

with $\boldsymbol{\varpi}_1(t) = 2\sum_{i=1}^N d_i \varphi_i(t) \zeta_i^T(t) \mathbf{P} \zeta_i^T(t)$ and $\boldsymbol{\varpi}_2(t) = \sum_{i=1}^N d_i (\varphi_i(t) - \alpha) \dot{\alpha}_i(t)$. Substituting Eq. into $\boldsymbol{\varpi}_1(t)$ gives

$$\begin{aligned} \boldsymbol{\varpi}_1(t) &= 2\zeta^T(t) [\boldsymbol{\phi}(t) \mathbf{D} \otimes \mathbf{P}] \zeta(t) \\ &= \zeta^T(t) [\boldsymbol{\phi}(t) \mathbf{D} \otimes (\mathbf{A}^T \mathbf{P} + \mathbf{P} \mathbf{A})] \zeta(t) \\ &\quad - \zeta^T(t) [\boldsymbol{\phi}(t) \bar{\mathbf{L}}_1 \boldsymbol{\phi}(t) \otimes \mathbf{P} \mathbf{B} \mathbf{B}^T \mathbf{P}] \zeta(t) \\ &\quad - 2\gamma \zeta^T(t) [\boldsymbol{\phi}(t) \mathbf{D} \mathbf{L}_1 \otimes \mathbf{P} \mathbf{B}] \bar{\mathbf{g}}(t) \\ &\quad - 2\zeta^T(t) [\boldsymbol{\phi}(t) \mathbf{D} \mathbf{L}_1 \otimes \mathbf{P} \mathbf{B}] \sigma_\gamma(\bar{\mathbf{u}}_0) \end{aligned}$$

where $\bar{\mathbf{g}}(t) = [\mathbf{g}_1^T(t), \mathbf{g}_2^T(t), \dots, \mathbf{g}_N^T(t)]^T$ and $\bar{\mathbf{L}}_1 = \mathbf{D} \mathbf{L}_1 + \mathbf{L}_1^T \mathbf{D}$. On the one hand, according to the definition of $\mathbf{g}_i(t)$ in Eq. (17), we have $\zeta_i^T(t) \mathbf{P} \mathbf{B} \mathbf{g}_i(t) = \|\mathbf{B}^T \mathbf{P} \zeta_i(t)\|$ and $\zeta_i^T(t) \mathbf{P} \mathbf{B} \mathbf{g}_j(t) \leq \|\mathbf{B}^T \mathbf{P} \zeta_i(t)\|$ for $i \neq j$, $i, j = 1, 2, \dots, N$. We then have

$$\begin{aligned} &- 2\gamma \zeta^T(t) [\boldsymbol{\phi}(t) \mathbf{D} \mathbf{L}_1 \otimes \mathbf{P} \mathbf{B}] \bar{\mathbf{g}}(t) \\ &= 2\gamma \sum_{i=1}^N d_i \varphi_i(t) \zeta_i^T(t) \mathbf{P} \mathbf{B} \left(\sum_{j=1}^N a_{ij} (\mathbf{g}_j(t) - \mathbf{g}_i(t)) - a_{i0} \mathbf{g}_i(t) \right) \\ &\leq -2\gamma \sum_{i=1}^N d_i a_{i0} \varphi_i(t) \|\mathbf{B}^T \mathbf{P} \zeta_i(t)\| \end{aligned}$$

Also, note that

$$\begin{aligned} -2\zeta^T(t) [\boldsymbol{\phi}(t) \mathbf{D} \mathbf{L}_1 \otimes \mathbf{P} \mathbf{B}] \sigma_\gamma(\bar{\mathbf{u}}_0) &= -2 \sum_{i=1}^N d_i a_{i0} \varphi_i(t) \zeta_i^T(t) \mathbf{P} \mathbf{B} \sigma_\gamma(\bar{\mathbf{u}}_0) \\ &\leq 2\gamma \sum_{i=1}^N d_i a_{i0} \varphi_i(t) \|\mathbf{B}^T \mathbf{P} \zeta_i(t)\| \end{aligned}$$

Substituting the above inequalities into $\boldsymbol{\varpi}_1(t)$ gives

$$\begin{aligned} \boldsymbol{\varpi}_1(t) &\leq \zeta^T(t) [\boldsymbol{\phi}(t) \mathbf{D} \otimes (\mathbf{A}^T \mathbf{P} + \mathbf{P} \mathbf{A})] \zeta(t) \\ &\quad - \zeta^T(t) [\boldsymbol{\phi}(t) \bar{\mathbf{L}}_1 \boldsymbol{\phi}(t) \otimes \mathbf{P} \mathbf{B} \mathbf{B}^T \mathbf{P}] \zeta(t) \\ &\leq \zeta^T(t) [\boldsymbol{\phi}(t) \mathbf{D} \otimes (\mathbf{A}^T \mathbf{P} + \mathbf{P} \mathbf{A})] \zeta(t) \\ &\quad - \bar{\lambda}_{\min} \zeta^T(t) [\boldsymbol{\phi}^2(t) \otimes \mathbf{P} \mathbf{B} \mathbf{B}^T \mathbf{P}] \zeta(t) \end{aligned} \quad (20)$$

where $\bar{\lambda}_{\min}$ is the minimum eigenvalue of $\bar{\mathbf{L}}_1$.

Since $\dot{\alpha}_i(t) = \zeta_i^T(t) \mathbf{P} \mathbf{B} \mathbf{B}^T \mathbf{P} \zeta_i(t)$, it follows that

$$\boldsymbol{\varpi}_2(t) = \zeta^T(t) [(\boldsymbol{\phi}(t) - \alpha \mathbf{I}_N) \mathbf{D} \otimes \mathbf{P} \mathbf{B} \mathbf{B}^T \mathbf{P}] \zeta(t) \quad (21)$$

It holds from Eq. (20) and Eq. (21) that

$$\begin{aligned} \dot{V}_\zeta(t) &= \boldsymbol{\varpi}_1(t) + \boldsymbol{\varpi}_2(t) \\ &\leq \zeta^T(t) [\boldsymbol{\phi}(t) \mathbf{D} \otimes (\mathbf{A}^T \mathbf{P} + \mathbf{P} \mathbf{A} + \mathbf{P} \mathbf{B} \mathbf{B}^T \mathbf{P})] \zeta(t) \\ &\quad - \zeta^T(t) [(\bar{\lambda}_{\min} \boldsymbol{\phi}^2(t) + \alpha \mathbf{D}) \otimes \mathbf{P} \mathbf{B} \mathbf{B}^T \mathbf{P}] \zeta(t) \end{aligned}$$

Select α large enough such that $\alpha \geq d_M / \bar{\lambda}_{\min}$ with $d_M = \max\{d_1, d_2, \dots, d_N\}$. We have

$$\begin{aligned} &-\zeta^T(t) [(\bar{\lambda}_{\min} \boldsymbol{\phi}^2(t) + \alpha \mathbf{D}) \otimes \mathbf{P} \mathbf{B} \mathbf{B}^T \mathbf{P}] \zeta(t) \\ &\leq -2\zeta^T(t) [\boldsymbol{\phi}(t) \mathbf{D} \otimes \mathbf{P} \mathbf{B} \mathbf{B}^T \mathbf{P}] \zeta(t) \end{aligned} \quad (22)$$

It follows from Eq. (22) that

$$\begin{aligned} \dot{V}_\zeta(t) &\leq \zeta^T(t) [\boldsymbol{\phi}(t) \mathbf{D} \otimes (\mathbf{A}^T \mathbf{P} + \mathbf{P} \mathbf{A} - \mathbf{P} \mathbf{B} \mathbf{B}^T \mathbf{P})] \zeta(t) \\ &= -\varepsilon \zeta^T(t) [\boldsymbol{\phi}(t) \mathbf{D} \otimes \mathbf{I}_n] \zeta(t) \leq 0 \end{aligned} \quad (23)$$

which implies that $V_\zeta(t)$ is bounded, and so is $\alpha(t)$. Note that $\dot{V}_\zeta(t) \equiv 0$ means $\zeta(t) = \mathbf{0}$, thus, we have $\lim_{t \rightarrow \infty} \zeta(t) = \mathbf{0}$ and

$\lim_{t \rightarrow \infty} \tilde{\mathbf{x}}_i(t) = \lim_{t \rightarrow \infty} (\mathbf{x}_i(t) - \mathbf{x}_0(t)) = \mathbf{0}$, since $\zeta(t) = (\mathbf{L}_1 \otimes \mathbf{I}_n) \tilde{\mathbf{x}}_i(t)$ and \mathbf{L}_1 is nonsingular. By Eq. (16), because $\alpha_i(t)$ is non-decreasing, it can be verified that $\alpha_i(t)$ converges to a certain positive constant. This completes the proof of [Theorem 2](#). ■

Remark 2. The result of Hua et al.²⁰ takes the control input of the leader agent into consideration as well. The observer in Hua et al.²⁰ (Eq. (4–1)) is constructed in a fully distributed way to estimate the state of the leader agent. It, however, cannot be directly applied to solve our problem because of the lack of the input matrix \mathbf{B} in the second term of the observer. Compared to Hua et al.²⁰ we consider the input saturation of followers, which is more practical. The consensus protocol is designed by combing the distributed observer in Hua et al.²⁰ and the low gain feedback design technique of Lin.¹³

3.3. Formation control of a multi-UAV system

In this subsection, we show how to convert a formation problem into the state consensus problem. Assume that each UAV is modeled as a double-integrator system (2) and the formation problem is considered in a 2-D plane, then the matrices \mathbf{A} , \mathbf{B} of the system in Eq. (2). that represent each UAV are

$$\mathbf{A} = \begin{bmatrix} \mathbf{0}_{2 \times 2} & \mathbf{I}_2 \\ \mathbf{0}_{2 \times 2} & \mathbf{0}_{2 \times 2} \end{bmatrix}, \mathbf{B} = \begin{bmatrix} \mathbf{0}_{2 \times 2} \\ \mathbf{I}_2 \end{bmatrix} \quad (24)$$

Let $\mathbf{p}_{di} \in \mathbf{R}^2$ be the desired constant relative position between the i th follower UAV and the leader UAV. Then, the objective of the formation control problem is to achieve

$$\lim_{t \rightarrow \infty} (\mathbf{p}_i(t) - \mathbf{p}_0(t)) = \mathbf{p}_{di}, \quad \lim_{t \rightarrow \infty} (\mathbf{v}_i(t) - \mathbf{v}_0(t)) = \mathbf{0}$$

Define the consensus error of each follower as

$$\mathbf{e}_i(t) := \begin{bmatrix} \mathbf{p}_i(t) - \mathbf{p}_{di} \\ \mathbf{v}_i(t) \end{bmatrix} - \begin{bmatrix} \mathbf{p}_0(t) \\ \mathbf{v}_0(t) \end{bmatrix}$$

Then, the system of each follower UAV is in the form of Eq. (2) with the state $[(\mathbf{p}_i(t) - \mathbf{p}_{di})^T, \mathbf{v}_i^T(t)]^T$, while the dynamics of the leader UAV remain unchanged. That is,

$$\begin{cases} \begin{bmatrix} \dot{\mathbf{p}}_0(t) \\ \dot{\mathbf{v}}_0(t) \end{bmatrix} = \begin{bmatrix} \mathbf{0}_{2 \times 2} & \mathbf{I}_2 \\ \mathbf{0}_{2 \times 2} & \mathbf{0}_{2 \times 2} \end{bmatrix} \begin{bmatrix} \mathbf{p}_0(t) \\ \mathbf{v}_0(t) \end{bmatrix} + \begin{bmatrix} \mathbf{0}_{2 \times 2} \\ \mathbf{I}_2 \end{bmatrix} \mathbf{a}_0(t) \\ \begin{bmatrix} \dot{\mathbf{p}}_i(t) - \dot{\mathbf{p}}_{di} \\ \dot{\mathbf{v}}_i(t) \end{bmatrix} = \begin{bmatrix} \mathbf{0}_{2 \times 2} & \mathbf{I}_2 \\ \mathbf{0}_{2 \times 2} & \mathbf{0}_{2 \times 2} \end{bmatrix} \begin{bmatrix} \mathbf{p}_i(t) - \mathbf{p}_{di} \\ \mathbf{v}_i(t) \end{bmatrix} + \begin{bmatrix} \mathbf{0}_{2 \times 2} \\ \mathbf{I}_2 \end{bmatrix} \mathbf{a}_i(t), \\ i = 1, 2, 3, 4 \end{cases} \quad (25)$$

It can be verified that the formation control problem is solved if $\lim_{t \rightarrow \infty} \mathbf{e}_i = \mathbf{0}$. In [Section 4](#), we will use system (24) and (25) to verify the effectiveness of our control protocol.

4. Simulation and experiment results

In this section, we will give simulation and experiment to verify our control laws. Subsections 4.1 and 4.2 will show the results that verify the distributed static control protocol (5) and the distributed adaptive control protocol (15), respectively. The simulation part is given to solve the semi-global consensus

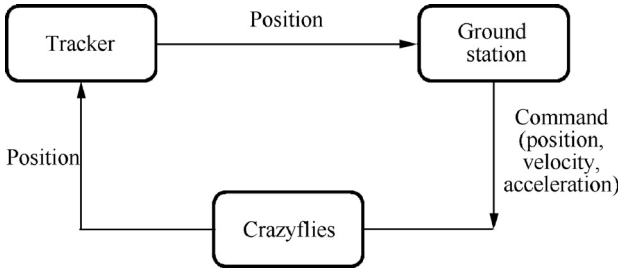


Fig. 2 Experimental setup for real flight tests of multiple UAVs.

problem with 1 leader and 4 followers, and real flight tests are showed to address the formation problem of a multi-UAV system using 1 leader UAV and multiple follower UAVs.

The real flight tests are done in a VICON room, and the data is obtained from the VICON motion capture system.²¹ We use Crazyflie 2.1,²² a nano quadrotor helicopter, as the experimental platforms. Fig. 2 above illustrates the experimental setup for our real flight tests with multiple UAVs.

Firstly, Tracker, a motion capture software, captures the positions of Crazyflies that are equipped with identifiable markers, and the data are sent to the ground station via the Robotic Operating System. In the ground station, our algorithm is implemented based on the Crazyswarm architecture,²³ which allows us to fly a swarm of quadcopters. The calculated position, velocity and acceleration are sent to Crazyflies via Crazyradio, to enable their built-in flight control laws to track the references generated from our control protocols.

4.1. Verification of the distributed static control

The simulation part solves the consensus problem stated in Problem 1 using the distributed static control protocol (5), with each agent is modeled as a double-integrator system. In this example, we assume that the input bounds of the leader and the followers are 1 and 3, respectively. It is easy to verify that Assumptions 1 and 2 are satisfied.

The communication topology is shown in Fig. 3. It is clear that the undirected graph satisfies Assumption 3. The Laplacian matrix L and the corresponding sub-matrix L_1 are

$$L = \begin{bmatrix} 0 & 0 & 0 & 0 & 0 \\ -1 & 3 & -1 & -1 & 0 \\ 0 & -1 & 2 & 0 & -1 \\ 0 & -1 & 0 & 1 & 0 \\ 0 & 0 & -1 & 0 & 1 \end{bmatrix}, L_1 = \begin{bmatrix} 3 & -1 & -1 & 0 \\ -1 & 2 & 0 & -1 \\ -1 & 0 & 1 & 0 \\ 0 & -1 & 0 & 1 \end{bmatrix}$$

respectively. It is straightforward to verify that L_1 is symmetric and positive definite.

For the distributed observer in Eq. (4) estimates that estimate the input bound of the leader UAV, the initial states of γ_i , $i = 1, 2, 3, 4$, are set as a random constants between (0,1), and the parameters are set as $\mu_1 = 1$ and $\rho = \frac{5}{7}$ since μ_1 is a positive constant and $1/2 < \rho < 1$, $\rho \in R_{odd}^+$. The estimation of γ is shown in Fig. 4. It can be seen that the estimation error $\gamma_i - \gamma$ converges to zero in a finite time.

The initial states of the leader agent and the follower agents are chosen as

$$[x_0(0), x_1(0), x_2(0), x_3(0), x_4(0)] = \begin{bmatrix} 1 & 0 & 0.8 & -1 & -1 \\ 1 & 2 & -1.2 & 2 & 1.7 \\ 0 & 0.3 & 0.6 & 1.2 & -0.4 \\ 0 & -0.5 & 0.2 & 0.8 & -1.2 \end{bmatrix}$$

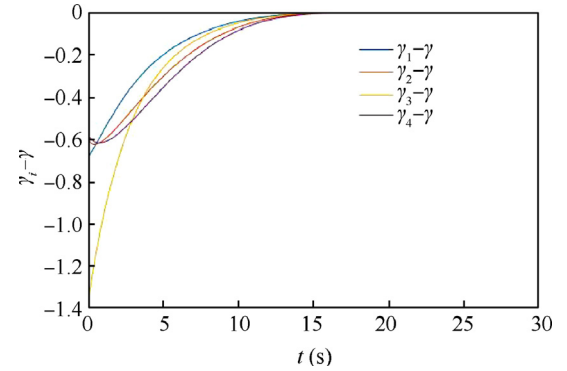


Fig. 4 Estimation of input bound of the leader UAV.

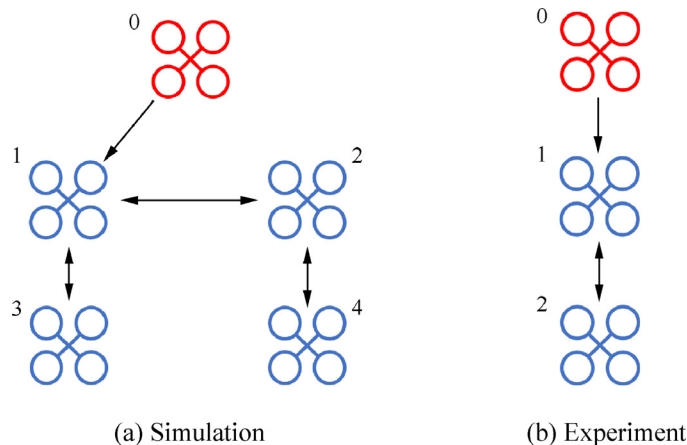


Fig. 3 Communication network \mathcal{G} in simulation and experiment of control protocol.

The input of the leader during the simulation process is demonstrated in the left figure of Fig. 5. It is obvious that it is within the input bound.

Now, we consider the low gain parameter $\varepsilon = 0.001$. The solution of the parameterized ARE Eq. (3) is

$$P(\varepsilon = 0.001) = \begin{bmatrix} 0.008 & 0 & 0.0316 & 0 \\ 0 & 0.008 & 0 & 0.0316 \\ 0.0316 & 0 & 0.2535 & 0 \\ 0 & 0.0316 & 0 & 0.2535 \end{bmatrix}$$

The states of all the agents and the consensus error are shown in Fig. 6. It is obvious that the leader-following consensus errors converge to zero asymptotically under the distributed static control protocol.

The flight test shows a formation control with the dynamics of the vehicles satisfying Eq. (25) using the distributed static control protocol (5). The topology is shown in Fig. 3(b). In this experiment, there is one leader UAV and two follower UAVs, and the communication graph among the followers is undirected. The initial states of the UAVs are set as

$$[\mathbf{x}_0(0), \mathbf{x}_1(0), \mathbf{x}_2(0)] = \begin{bmatrix} \mathbf{p}_0(0) & \mathbf{p}_1(0) & \mathbf{p}_2(0) \\ \mathbf{v}_0(0) & \mathbf{v}_1(0) & \mathbf{v}_2(0) \end{bmatrix} = \begin{bmatrix} 1 & -0.7 & 1.2 \\ 2.5 & 3.2 & 3.7 \\ 0 & 0 & 0 \\ 0 & 0 & 0 \end{bmatrix}$$

The desired relative distances between the 2 follower UAVs and the leader UAV are

$$\begin{cases} \mathbf{p}_{d1} = \mathbf{p}_1(t) - \mathbf{p}_0(t) = [-0.8, 1]^T \\ \mathbf{p}_{d2} = \mathbf{p}_2(t) - \mathbf{p}_0(t) = [0.8, 1]^T \end{cases}$$

Thus, the desired shape formed by the three UAVs is a triangle. Note that the initial position of the vehicles is not in the desired shape.

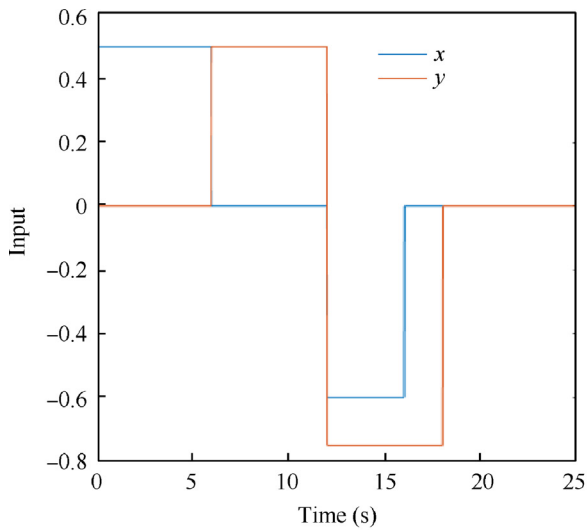
During the formation flight control, the acceleration of the leader is demonstrated in the right figure of Fig. 5, under which, the trajectory of each UAV is shaped like the letter 'Z'. It is obvious that the acceleration and velocity are within the boundary constraint of the vehicles. Other parameters used in the experiment are the same as the that in the simulation in the above part. During the flight, the vehicles firstly take off to the height of 1 m at a constant speed, then the control protocol starts to work to form the desired formation, after which they descend to the ground. The video of flight test can be found in <https://youtu.be/XLnpWv25eSw>. The comparison of trajectories in real flight and simulation is shown in Fig. 7. Fig. 8 demonstrates the tracking errors of each UAV between the real flight and simulation during the time the control protocol works, from which we find that the maximum tracking error between the experiment and simulation is about 29 cm. Combing the results in Fig. 7 and Fig. 8, it is not difficult to draw the conclusion that the UAVs asymptotically converge to the desired formation from the given initial condition under the distributed static control protocol (5). A further analysis of the result will be given in Remark 3.

4.2. Verification of the distributed adaptive control

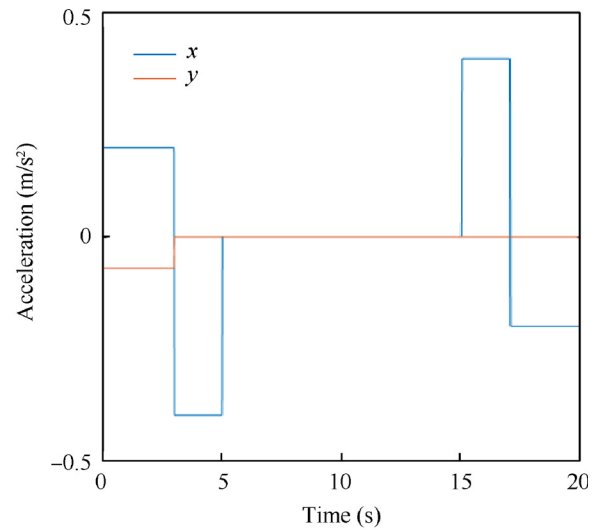
The simulation part solves the consensus problem stated in Problem 1 using the distributed adaptive control protocol (15), with each agent is modeled as a double-integrator system. In this example, we assume that the input bounds of the leader agent and the follower agents are 1 and 3, respectively, i.e., $\gamma = 1$, $\Delta = 3$. It is easy to verify that Assumptions 1 and 2 are satisfied.

The communication topology is shown in Fig. 9. It is clear that the directed graph satisfies Assumption 4.

The Laplacian matrix L of \mathcal{G} and the corresponding sub-matrix L_1 are



(a) Input of leader in simulation



(b) Acceleration of leader in flight test

Fig. 5 Input of leader in simulation and acceleration of leader in flight test of the control protocol (5).

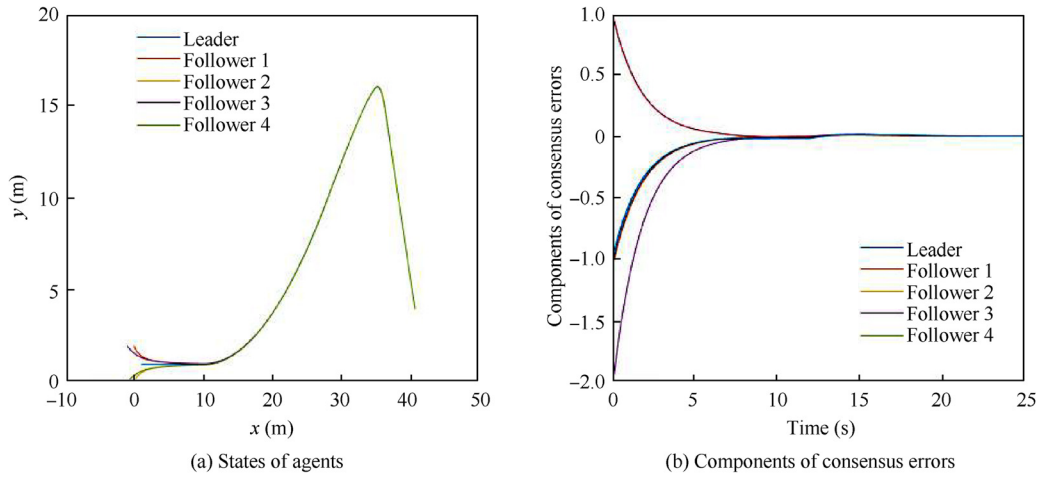


Fig. 6 States of the agents and consensus errors under the distributed static control protocol (5).

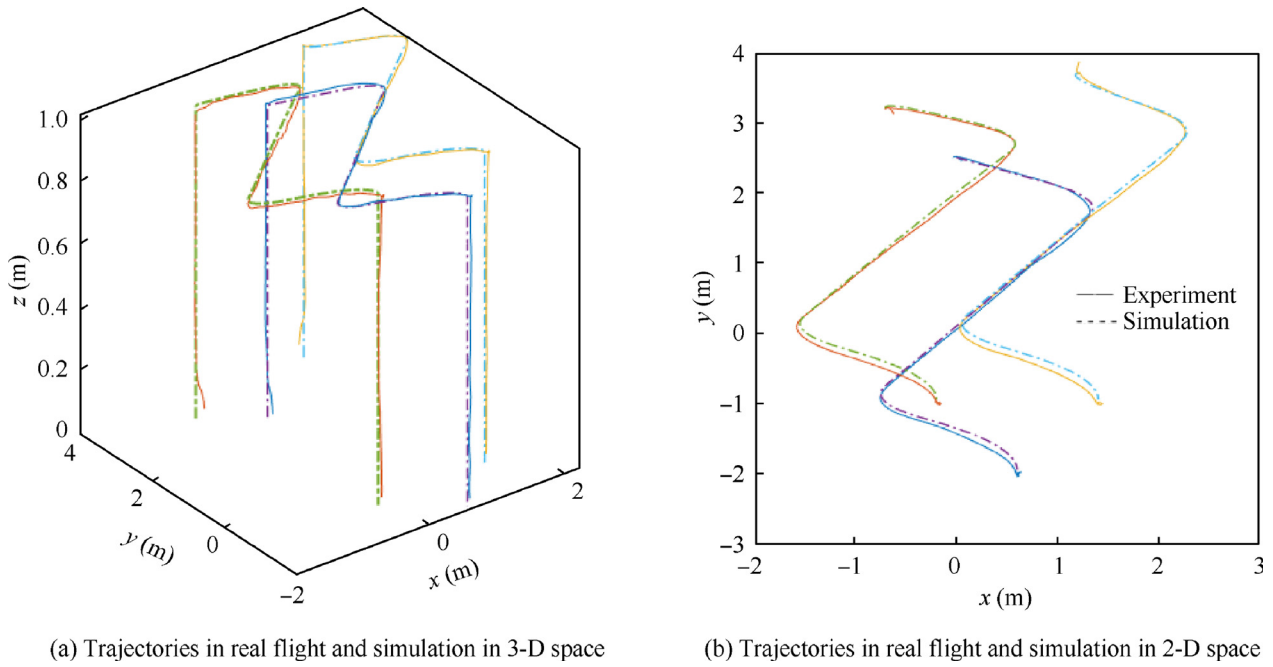


Fig. 7 Comparison of trajectories in real flight and simulation with distributed static control protocol (5).

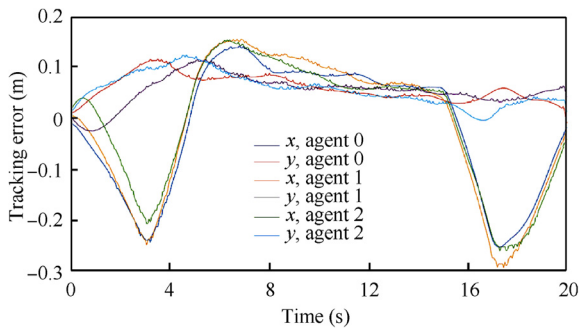


Fig. 8 Tracking error between the simulation and real flight test of the distributed static control protocol (5).

$$L = \begin{bmatrix} 0 & 0 & 0 & 0 & 0 \\ -1 & 1 & 0 & 0 & 0 \\ 0 & -1 & 1 & 0 & 0 \\ 0 & 0 & -1 & 1 & 0 \\ 0 & -1 & -1 & 0 & 2 \end{bmatrix}, \quad L_1 = \begin{bmatrix} 1 & 0 & 0 & 0 \\ -1 & 1 & 0 & 0 \\ 0 & -1 & 1 & 0 \\ -1 & -1 & 0 & 2 \end{bmatrix}$$

It is obvious that all eigenvalues of L_1 have positive real parts.

The initial state of the updating gain $\alpha_i(t)$ for every follower is set as $[\alpha_1(0), \alpha_2(0), \alpha_3(0), \alpha_4(0)] = [0.01, 0.02, 0.015, 0.02]$. The initial states of the leader agent and the follower agents are chosen as

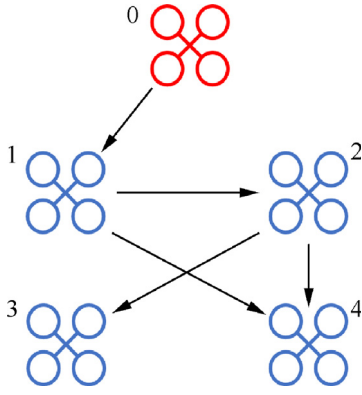


Fig. 9 Communication network \mathcal{G} used in both simulation and experiment of control protocol (15).

$$[\mathbf{x}_0(0), \mathbf{x}_1(0), \mathbf{x}_2(0), \mathbf{x}_3(0), \mathbf{x}_4(0)] = \begin{bmatrix} -1 & -1.8 & -0.2 & -1.4 & 0.2 \\ 2.5 & 3.5 & 3.5 & 3.5 & 3.5 \\ 0 & 0 & 0 & 0 & 0 \\ -0.25 & -0.3 & 0.2 & -0.2 & -1.2 \end{bmatrix}$$

The input of the leader agent during the simulation process is presented in the left figure of Fig. 10. We note that it is within the input bound.

We consider the low gain parameter $\varepsilon = 0.01$. The solution of the parameterized ARE in Eq. (3) is

$$P(\varepsilon = 0.01) = \begin{bmatrix} 0.0458 & 0 & 0.1 & 0 \\ 0 & 0.0458 & 0 & 0.1 \\ 0.1 & 0 & 0.4583 & 0 \\ 0 & 0.1 & 0 & 0.4583 \end{bmatrix}$$

In Fig. 11, the trajectories $\mathbf{p}_i(t)$ and consensus errors e_i , $i = 1, 2, 3, 4$, are given, where we can conclude that the consensus errors converge to zero asymptotically under the dis-

tributed adaptive control protocol. The values of the updating gain $\alpha_i(t)$ for every follower is shown in Fig. 12. We can find that each $\alpha_i(t)$ converges to a positive constant.

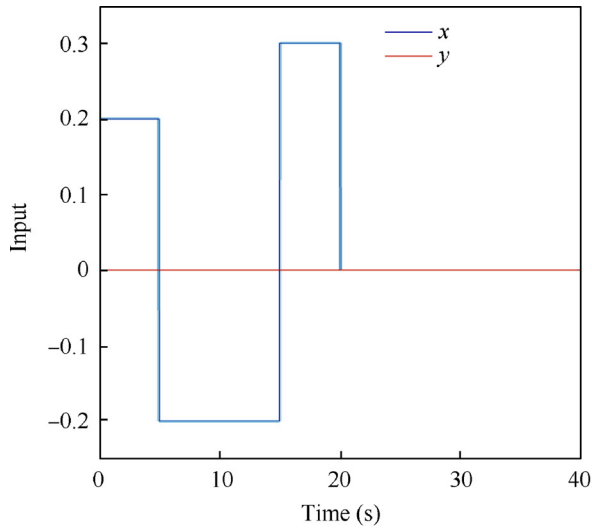
The flight test shows a formation control with the dynamics of the vehicles satisfying using the distributed static control protocol (5) under the topology Fig. 9. The initial states of the UAVs are set as

$$[\mathbf{x}_0(0), \mathbf{x}_1(0), \mathbf{x}_2(0), \mathbf{x}_3(0), \mathbf{x}_4(0)] = \begin{bmatrix} 0 & -0.6 & 0.4 & -0.1 & 0.8 \\ 2 & 2.5 & 2.7 & 3 & 3 \\ 0 & 0 & 0 & 0 & 0 \\ 0 & 0 & 0 & 0 & 0 \end{bmatrix}$$

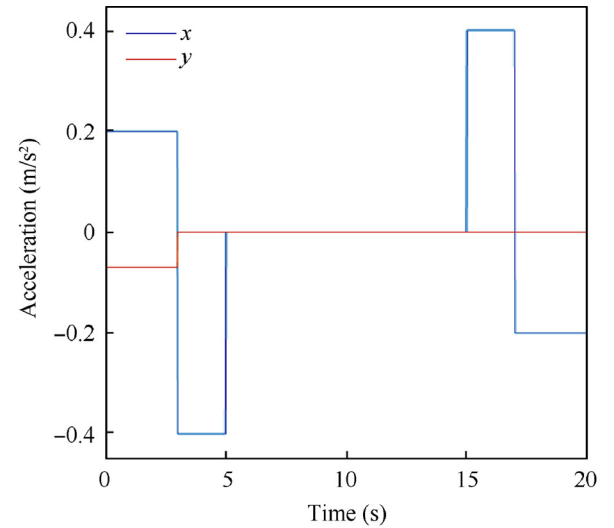
The relative distance between the 4 follower UAVs and the leader UAV is

$$\begin{cases} \mathbf{p}_{d1} = \mathbf{p}_1(t) - \mathbf{p}_0(t) = [-0.5, 0.6]^T \\ \mathbf{p}_{d2} = \mathbf{p}_2(t) - \mathbf{p}_0(t) = [0.5, 0.6]^T \\ \mathbf{p}_{d3} = \mathbf{p}_3(t) - \mathbf{p}_0(t) = [-0.5, 1.2]^T \\ \mathbf{p}_{d4} = \mathbf{p}_4(t) - \mathbf{p}_0(t) = [0.5, 1.2]^T \end{cases}$$

Note that the initial position of the vehicles is not in the desired formation. During the formation flight control, the acceleration of the leader agent is the same as that in the former test, and other parameters used in the experiment are the same as that in the simulation in the above part. Similar to the former test, the control protocol works when the UAVs are at the height of 1 m. The video of flight test can be found in <https://youtu.be/6SNDqtqWYZg>. The comparison of trajectories in real flight and simulation is shown in Fig. 13, while Fig. 14 illustrates the tracking errors of each UAV between the real flight and simulation during the time the control protocol works, from which we find that the maximum tracking error between the experiment and simulation is about 19 cm. Combing the results in Fig. 13 and Fig. 14, it is easy to draw the conclusion that given the initial condition, the UAVs converge to the desired formation asymptotically under the distributed adaptive control protocol (15).



(a) Input of leader in simulation



(b) Acceleration of leader in flight test

Fig. 10 Input of leader in simulation and acceleration of leader in flight test of control protocol (15).

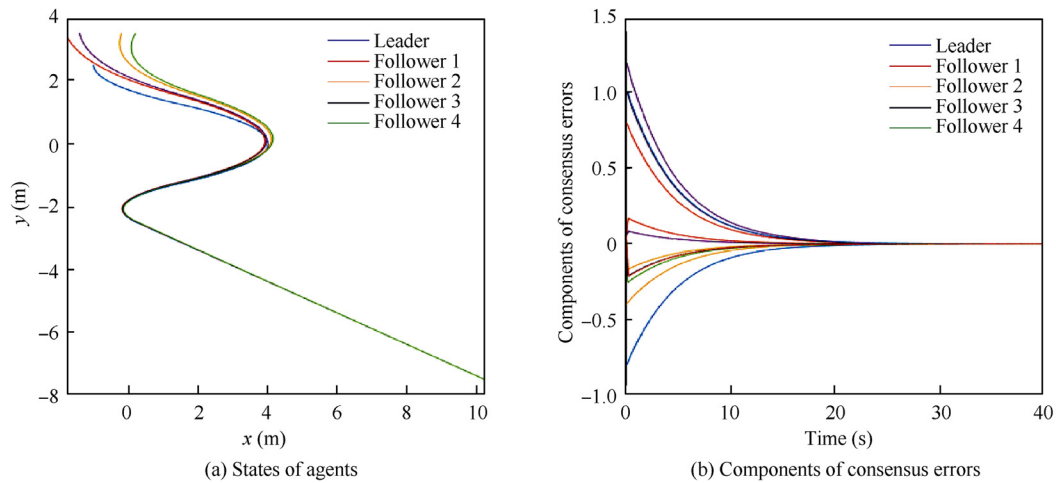


Fig. 11 States of the agents and consensus errors under the distributed adaptive control protocol (15).

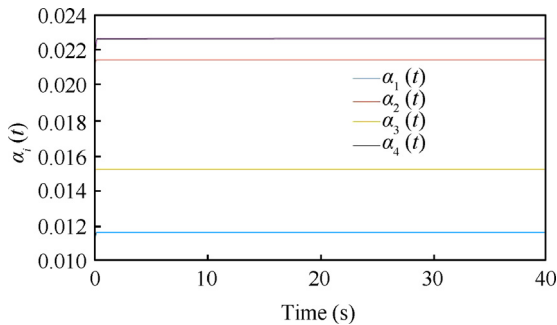
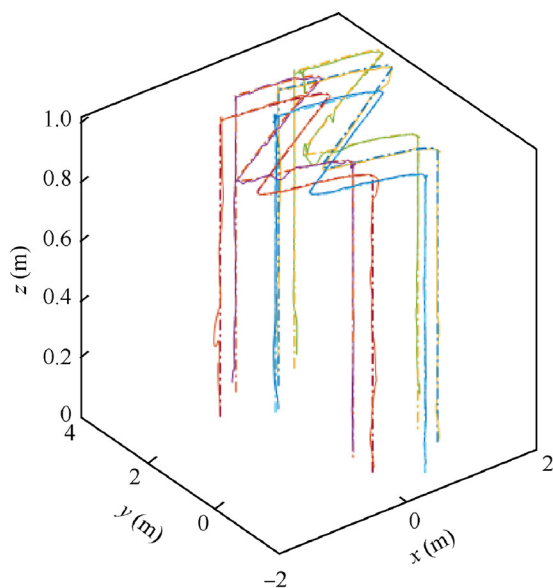
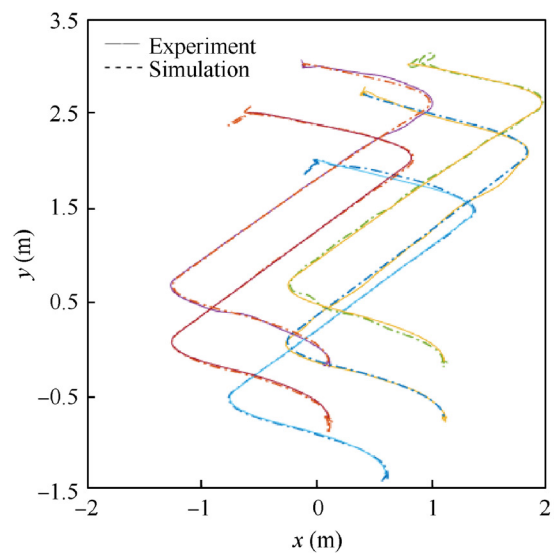


Fig. 12 Values of the updating gain in the distributed adaptive control protocol (15).

Remark 3. We note that the vehicles cannot track the trajectory perfectly and there are some oscillations of Crazyflies during the flight process as the videos shows. There are two main reasons for this fact. First, the dynamics of Crazyflies cannot be exactly expressed by double-integrator systems. The dynamics of Crazyflies²² is more complex than the systems we used. Second, the hardware of Crazyflies and the instability of the VICON motion capture system will affect the experiment result to a certain degree. As Fig. 15 illustrates, there remains tracking error during the takeoff phase where the control protocol does not work. Though the tracking error cannot be completely eliminated, it is within the acceptable limits. However, it does not affect the verification of our control law. It is worth noting that the multiple vehicles finally converge to the desired formation from the given initial



(a) Trajectories in real flight and simulation in 3-D space



(b) Trajectories in real flight and simulation in 2-D space

Fig. 13 Comparison of trajectories in real flight and simulation with distributed adaptive control protocol (15).

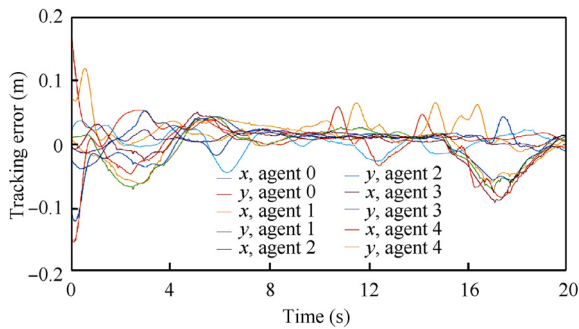


Fig. 14 Tracking error between the simulation and real flight test of the distributed adaptive control protocol (15).

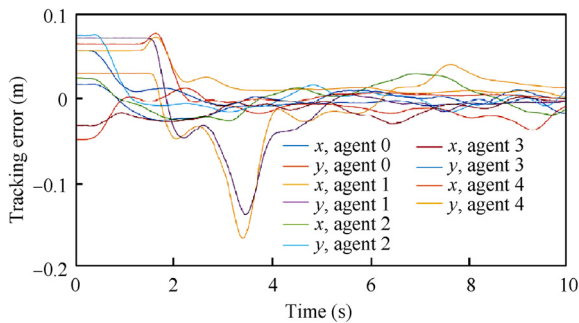


Fig. 15 Tracking errors of UAVs during the takeoff phase.

position, under the distributed static control law and the distributed adaptive control law.

5. Conclusions

We have investigated in this work the formation control of multiple UAVs based on the semi-global leader-following consensus method. Two consensus protocols, i.e., the distributed static control protocol and the distributed adaptive control protocol, have been proposed and verified. The distributed static control protocol is applicable to undirected topologies and it depends on the global information of the communication graph, while the distributed adaptive control protocol is designed over directed topologies and an updating gain is used to make it fully distributed with only neighbor interaction. Via the low gain feedback design technique, the semi-global leader-following consensus problem is solved by our proposed protocols if the leader agent is globally reachable. Finally, a formation control problem of UAVs is formulated into the consensus problem, and real flight tests are done to verify the effectiveness of our control protocols.

Declaration of Competing Interest

The authors declare that they have no known competing financial interests or personal relationships that could have appeared to influence the work reported in this paper.

Acknowledgements

This work is supported in part by the Research Grants Council of Hong Kong SAR, China (No.14209020) and in part by Peng Cheng Laboratory, China.

References

- Rastgoftar H, Taheri E, Ghasemi AH, et al. Continuum deformation of a multi-quadcopter system in a payload delivery mission. *IFAC-Papers OnLine* 2017;**50**(1):3455–62.
- Liu Y, Liu Z, Shi J, et al. Optimization of base location and patrol routes for unmanned aerial vehicles in border intelligence, surveillance, and reconnaissance. *J Adv Transp* 2019;**2019**:9063232. <https://doi.org/10.1155/2019/9063232>.
- Zhou P, Chen B. M. Formation-containment control of Euler-Lagrange systems of leaders with bounded unknown inputs. *IEEE Transactions on Cybernetics*. 2020; <https://doi.org/10.1109/TCYB.2020.3034931>.
- Liang Y, Dong Q, Zhao Y. Adaptive leader–follower formation control for swarms of unmanned aerial vehicles with motion constraints and unknown disturbances. *Chin J Aeronaut* 2020;**33**(11):2972–88.
- Wang Y, Zhang T, Cai Z, et al. Multi-UAV coordination control by chaotic grey wolf optimization based distributed MPC with event-triggered strategy. *Chin J Aeronaut* 2020;**33**(11):2877–97.
- Abdessameud A, Tayebi A. Formation control of VTOL unmanned aerial vehicles with communication delays. *Automatica* 2011;**47**(11):2383–94.
- Seo J, Kim Y, Kim S, et al. Consensus-based reconfigurable controller design for UAV formation fight. *Proceedings of the Institute of Mechanical Engineers, Part G: Journal of Aerospace Engineering* 2012; **226**(7): 817–29.
- Turpin M, Michael N, Kumar V. Decentralized formation control with variable shapes for aerial robots. *Proceedings of the 2012 IEEE international conference on robotics and automation*; 2012 May 14–18; RiverCentre, Saint Paul, Minnesota, USA. Piscataway: IEEE Press; 2012. p. 23–30.
- Dong X, Hu G. Time-varying formation tracking for linear multiagent systems with multiple leaders. *IEEE Trans Autom Control* 2017;**62**(7):3658–64.
- Semsar-Kazeroni E, Khorasani K. Optimal consensus algorithms for cooperative team of agents subject to partial information. *Automatica* 2008;**44**(11):2766–77.
- Qian Y, Liu L, Feng G. Output consensus of heterogeneous linear multi-agent systems with adaptive event-triggered control. *IEEE Trans Autom Control* 2019;**24**(6):2627–40.
- Lin Z, Stoorvogel AA, Saberi A. Output regulation for linear systems subject to input saturation. *Automatica* 1996;**32**(1):29–47.
- Lin Z. *Low gain feedback*. Berlin: Springer; 1999.
- Shi L, Li Y, Lin Z. Semi-global leader-following output consensus of heterogeneous multi-agent systems with input saturation. *Int J Robust Nonlinear Control* 2018;**28**(16):4916–30.
- Zhao Z, Hong Y, Lin Z. Semi-global output consensus of a group of linear systems in the presence of external disturbances and actuator saturation: An output regulation approach. *Int J Robust Nonlinear Control* 2016;**26**(7):1353–75.
- Cai G, Chen BM, Lee TH. *Unmanned rotorcraft systems*. Berlin: Springer; 2011.
- Li Z, Ren W, Liu X, et al. Distributed containment control of multi-agent systems with general linear dynamics in the presence of multiple leaders. *Int J Robust Nonlinear Control* 2013;**23**(5):534–47.
- Cai M, Xiang Z. Adaptive finite-time consensus tracking for multiple uncertain mechanical systems with input saturation. *Int J Robust Nonlinear Control* 2017;**27**(9):1653–76.

19. Qu Z. *Cooperative control of dynamical systems: Applications to autonomous vehicles*. Berlin: Springer; 2009.
20. Hua Y, Dong X, Hu G, et al. Distributed time-varying output formation tracking for heterogeneous linear multiagent systems with a nonautonomous leader of unknown input. *IEEE Trans Autom Control* 2019;**64**(10):4292–9.
21. Vicon motion capture systems [Internet]. [cited 2021 January 20]. Available from: <http://www.vicon.com/>.
22. Crazyflie 2.0 [Internet]. [cited 2021 January 20]. Available from: <https://www.bitcraze.io/products/crazyflie-2-1/>.
23. Preiss J, Honig W, Sukhatme G, et al. Crazyswarm: A large nano-quadcopter swarm. *2017 IEEE international conference on robotics and automation*; 2017 May 29-June 3; Singapore, Singapore. Piscataway: IEEE Press; 2017.p. 3299-304.